VA RESEARCH & DEVELOPMENT

JRRD
Journal of Rehabilitation Research & Development
Vol. 36 No. 3, July 1999

# Three-dimensional Foot Modeling and Analysis of Stresses in Normal and Early Stage Hansen's Disease with Muscle Paralysis

**Shanti Jacob, PhD and Mothiram K. Patil, DSc**

*Biomedical Engineering Division, Department of Applied Mechanics, Indian Institute of Technology, Madras-600 036*

**Abstract**--The models of the foot available in the literature are either two- or three-dimensional (3-D), representing a part of the foot without considering different segments of bones, cartilages, ligaments, and important muscles. Hence, there is a need to develop a 3-D model with sufficient details. In this paper, a 3-D, two-arch model of the foot is developed, taking foot geometry from the X-rays of nondisabled controls and a Hansen's disease (HD) subject, and taking into consideration bones, cartilages, ligaments, important muscle forces, and foot sole soft tissue. The stress analysis is carried out by finite element (FE) technique using NISA software for the foot models, simulating quasi-static walking phases of heel-strike, mid-stance, and push-off. The analysis shows that the highest stresses occur during push-off phase in the dorsal central part of the lateral and medial metatarsals, the dorsal junction of the calcaneus, and the cuboid and plantar central part of the lateral metatarsals in the foot. The stresses in push-off phase in critical tarsal bone regions, for the early stage of HD with muscle paralysis, increase by 25-50% as compared with the control foot model. The model calculated stress results at the plantar surfaces are of the same order of magnitude as the measured foot pressures (0.2-0.5 MPa). The high stress concentration areas in the foot bones indicated above are of great importance, since it is found from clinical reports that in some subjects with pathogenic decrease in the mechanical strength of the bone from HD, these areas of bone are disintegrated. Therefore, this investigation could possibly provide an insight into the factors contributing to disintegration of tarsal bones in HD.

**Key words:** *early stage Hansen's disease, foot sole soft tissue, muscle paralysis, stress analysis,*

*two-arch foot model.*

## INTRODUCTION

The bone changes and paralysis of foot muscles occurring in Hansen's disease (HD) or diabetes are found to alter the pattern of internal stresses in the foot. As HD advances, its paralytic effects cause changes in the geometry as well as in the actions of muscle forces, giving rise to an increase in stresses at some sites and possibly causing tarsal disintegration when the mechanical strength in those regions is decreased. Direct measurements of the internal stresses are not possible *in vivo.* However, these stresses can be predicted using an appropriate numerical model of the foot acted upon by the important muscles. The analysis is first done on the foot of a nondisabled control followed by the analysis on the foot of a person with HD, with early bone changes and foot drop caused by the paralysis of certain muscles.

The foot models available (1-5) for stress analysis are two dimensional. The few three-dimensional (3-D) models available for stress analysis (6-11) represented only part of the foot skeleton and do not consider actual geometry or the role of ligaments, cartilages, and foot sole soft tissue. Therefore, it is found to be necessary to develop a 3-D model of the foot, taking into consideration all the above details, along with important muscle forces and the actual geometry of the foot.

This paper describes a 3-D, two-arch model of a control foot, taking into consideration the actual geometry of foot bone segments, cartilages, ligaments, foot sole soft tissue, and important muscle forces, for stress analysis during quasi-static walking phases of heel-strike, mid-stance, and push-off. Once the areas of high stress concentration are determined, the study is extended to model the foot of a person with HD to find the combined effect of early bone changes and muscle paralysis on the pattern of stresses developed.

## METHODS

### Foot Model

*Normal Foot with Foot Sole Soft Tissue*

The 3-D model of the foot, consisting of two arches (the medial and the lateral) with the soft tissue of the foot sole, is developed to simulate quasi-static walking phases of heel-strike, mid-stance, and push-off. The geometry of the foot is taken from medio-lateral and antero-posterior X-ray pictures of a control foot. In both arches, the individual metatarsal bones in the medio-lateral directions (three in the medial and two in the lateral arch) are combined. The bones, with their respective cartilages, are constrained to move by their respective longitudinal ligaments, modeled both on dorsal and plantar sides, and these ligaments are distributed in the medio-lateral direction as per anatomical data (12,13). The complex cartilage between calcaneus and talus is also introduced with medial, lateral, cervical, and interosseous ligaments. Ligaments are provided to

connect the medial arch and lateral arch in their respective places, as are the important plantar ligaments, such as spring ligaments, long plantar ligaments, and plantar facia (12-14). These ligaments are also distributed over a large area as found in the anatomy of the foot. Thus, the model consists of eight cartilages between the bones, each with its respective ligaments. The predominant muscle forces acting on the foot are taken into consideration per the literature (15,16), and the points of insertion of the muscles on the model are decided considering the anatomical data (12-14). The forces in the muscles attached to the lateral arch are also modeled in this two-arch model. The thicknesses of the soft tissue used (heel=18 mm; metatarsal heads=13 mm) conform to thicknesses reported in literature (17,18). The soft tissue of the plantar side alone is modeled.

**Figure 1** shows two views of the geometry of the skeleton along with that of the sole soft tissue in the medio-lateral view. The soft tissue under the medial arch is modeled with an arch shape as seen in a normal foot. The bottom surface of the soft tissue of lateral arch is modeled as a plane touching the ground.

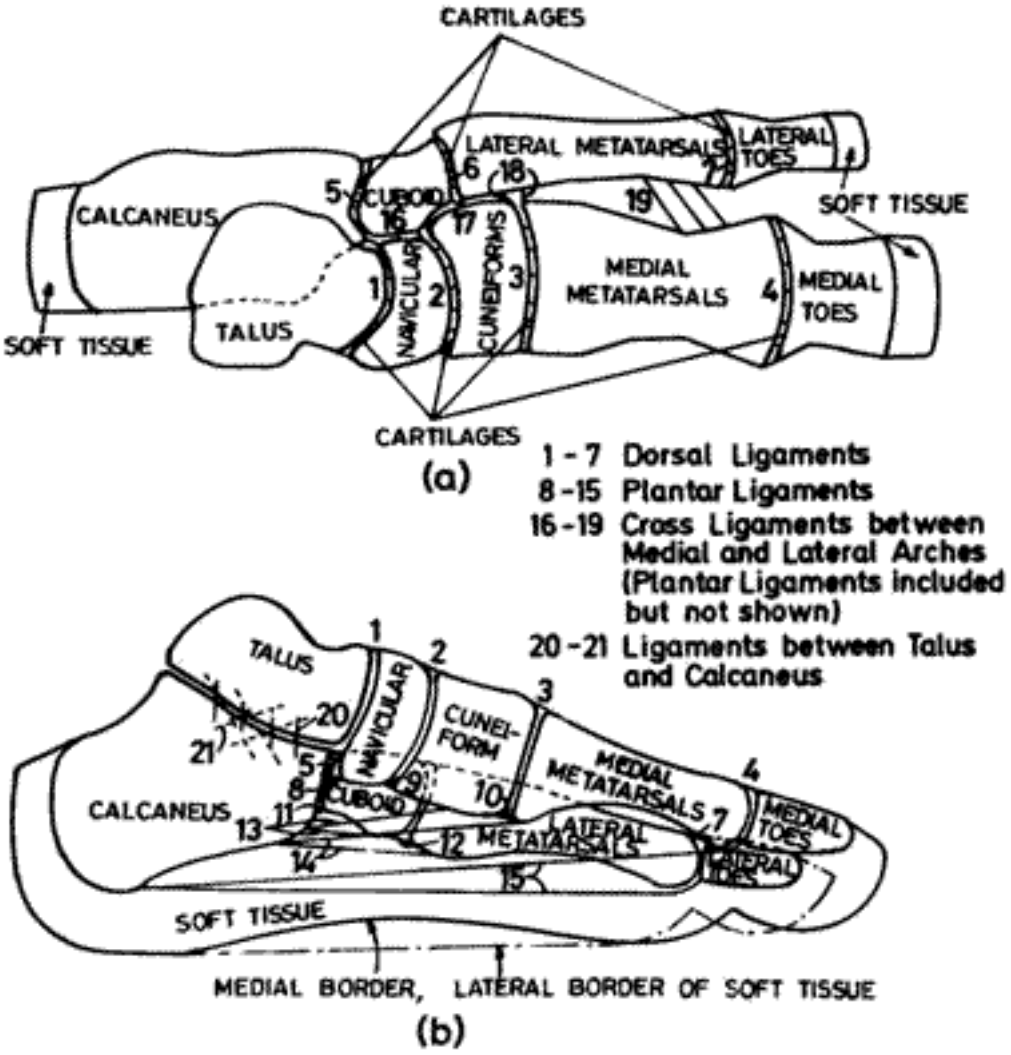


**Figure 1.**
Schematic diagram of the left foot skeleton, with plantar soft tissue; a=dorsal view; b=medial view.

Huiskes and Chao (19) have reported that in the case of quasi-static loading (and probably *in vivo* loading), both cortical and trabecular bones behave approximately in a linear elastic manner. In a recent work, Keaveny et al. (20,21) have reported that trabecular bone is linearly elastic until yielding and has equal tensile and compressive moduli. These elastic and yield properties are also characteristic of cortical bone (22-24). Although no Young's modulus data seem to be available specifically for the foot bones, values measured for various bones of arm and leg show little difference (25), so a value in this range can reasonably be chosen. Clift (26) has reported that under short-term or instantaneous loading, some useful information can be gained by modelling the cartilage as a linear elastic material. The stress-strain relationship for ligaments show nonlinear effects for very small loading, followed by a linear portion that applies over the range of normal physiological loadings (27). Hence, in this study, the foot bone material, cartilage, and ligaments are assumed to be homogeneous, isotropic, and linearly elastic. The Young's modulus of the bone is taken as 7,300 MPa and Poisson's ratio as 0.3 from Nakamura (1); those of the cartilage are taken as 10 MPa and 0.4, respectively, from Schreppers (28). The stiffness of the ligaments is taken as 1,500 N/mm from Patil (4).

The transfer of load to soft tissue using the elasticity theory has been studied by Bennet (29-31), who investigated soft tissue failure and dermatological problems experienced in fitting prosthetic devices to persons with amputation. Although he realized that there are numerous complexities in real tissues and variations with anatomical locations, in order to simplify the analysis to manageable proportions, he assumed a constant Young's modulus and Poisson's ratio for soft tissue. Similar assumptions are made by different investigators (10,11,32). Hence, in this study the foot sole soft tissue is assumed to be linearly elastic with a constant Poisson's ratio (to reduce complications) as done by other investigators (10,11,29-32). The Young's modulus of the soft tissue is taken as 1 MPa (32) and the Poisson's ratio as 0.49, that is, nearly incompressible (1).

The foot model is discretized into eight-node, isoparametric, solid brick elements and six-node wedge elements representing the bones, cartilages, and soft tissue, and into two-node spring elements representing the ligaments. The elements have three translational degrees of freedom per node, defined by first order interpolation functions, and the state of stress is characterized by six stress components. The governing mathematical equations--strain-displacement, stress-strain, and equilibrium equations for the 3-D model involving finite elements (FE)--are given in Zienkiewicz (33) and therefore not discussed here. The stress analyses are carried out using the commercial software, Numerically Integrated Elements for System Analysis, (NISA; Engineering Mechanics Research Corporation, Troy, MI).

*Heel-strike Phase*

The heel-strike phase is characterized by a 30° inclination of the foot sole to the ground (34). The ankle joint force (FAN) is simulated by 2.25 times the body weight (35). The muscles modeled in this phase of walking are tibialis anterior (TA), extensor hallucis longus (EHL), and extensor digitorum longus (EDL; 15,16). The inferior extensor retinaculum transfers the forces of TA, EHL, and EDL to the medial and lateral sides of the calcaneus and these forces are also considered in this model. The foot model (as seen from lateral side) in the heel-strike phase acted upon by the muscle forces and FAN is shown in **Figure 2.**

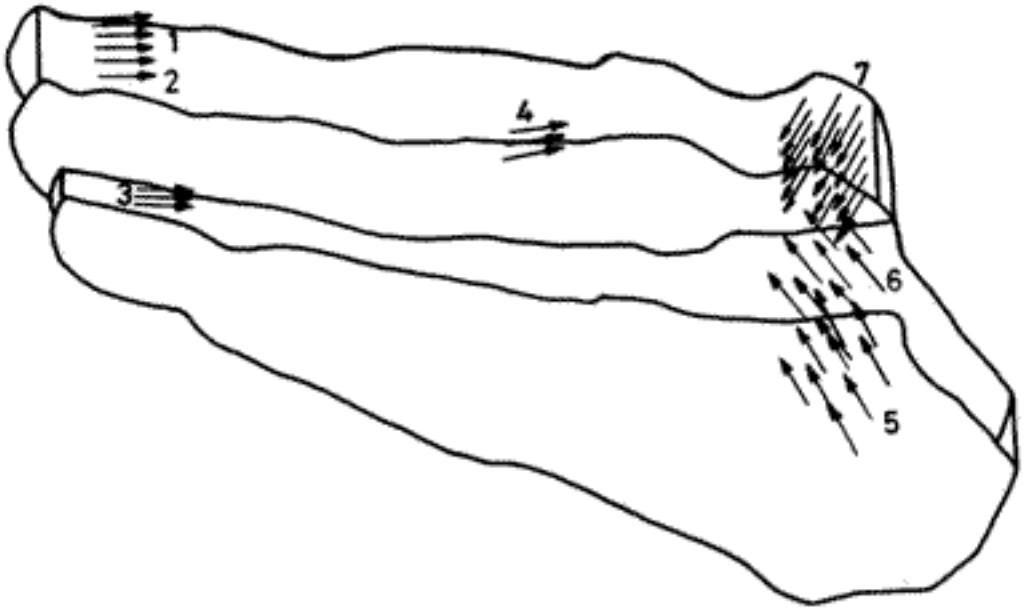


**Figure 2.**
Lateral view of the two-arch model of the foot with plantar soft tissue in the heel-strike phase. Acting forces are indicated by numbers 1-7: 1=EHL; 2=EDL in medial arch; 3=EDL in lateral arch; 4=TA; 5=reaction on the lateral side of the calcaneus due to retinaculum; 6=reaction on the medial side of the calcaneus due to retinaculum; 7=FAN. Forces 1-4 are distributed over thickness; 5-7 over area.

The forces in the above muscles are obtained from the literature (16,36,37) and by force equilibrium considerations; they are given in **Table 1.** The muscle attachments are not modeled as single points, but distributed over an area in conformity to the anatomy, to avoid stress concentrations at the attachment points of muscle forces. The FE mesh is the same as that used in the mid-stance phase (shown in the next section). The model in the heel-strike phase has 3,412 brick elements to represent bones, cartilages, and soft tissue, and 116 spring elements to represent ligaments, with a total of 4,557 nodes. The following boundary conditions are used in the heel-strike phase: the displacements at the medial border nodes of the heel region are arrested in the x, (=horizontal posterior-anterior), y (=vertical plantar-dorsal), and z (=horizontal lateral-medial) directions. The displacements at the lateral heel border nodes are arrested in the x and y directions, and the other nodes in the heel region are arrested in the y direction; virtual support is provided at the toes.

**Table 1.**

Muscle forces and ankle joint force acting on the two-arch foot model with soft tissue of the foot sole for control subject in different phases of walking.

| | Magnitude (N) | | |
|---|---|---|---|
| **Forces** | **Heel-strike** | **Mid-stance** | **Push-off** |

| | | | |
|---|---|---|---|
| Ankle Joint Force (FAN) | 1,350 | 2,100 | 3,000 |
| Triceps Surae (TS) | -- | 550 | 1,100 |
| Peroneus Longus (PL) | -- | 132 | 234 |
| Peroneus Brevis (PB) | -- | 64 | 96 |
| Tibialis Posterior (TP) | -- | 290 | 453 |
| Tibialis Anterior (TA) | 516 | -- | -- |
| Flexor Hallucis Longus (FHL) | -- | 143 | 259 |
| Flexor Digitorum Longus (FDL) | -- | 68 | 130 |
| Extensor Hallucis Longus (EHL) | 50 | -- | -- |
| Extensor Digitorum Longus(EDL) | 114 | -- | -- |
| Reaction at medial pulley due to muscle forces FHL, FDL, and TP | -- | 645 | 613 |
| Reaction at lateral pully due to muscle forces PL and PB | -- | 256 | 243 |
| Reaction on medial side of calcaneus due to retinaculum | 318 | -- | -- |
| Reaction on lateral side of calcaneus due to retinaculum | 318 | -- | -- |

*Mid-stance Phase*

The foot model shown in **Figure 3** represents the mid-stance phase, where the foot is supported at the heel and forefoot. The FAN is simulated by 3.5 times the body weight of a control subject (35) weighing 600 N. During the mid-stance phase, the muscles triceps surae (TS), peroneus longus (PL), peroneus brevis (PB), tibialis posterior (TP), flexor hallucis longus (FHL), flexor digitorum longus (FDL), and adductor hallucis (AH) are considered in this model (15,16).

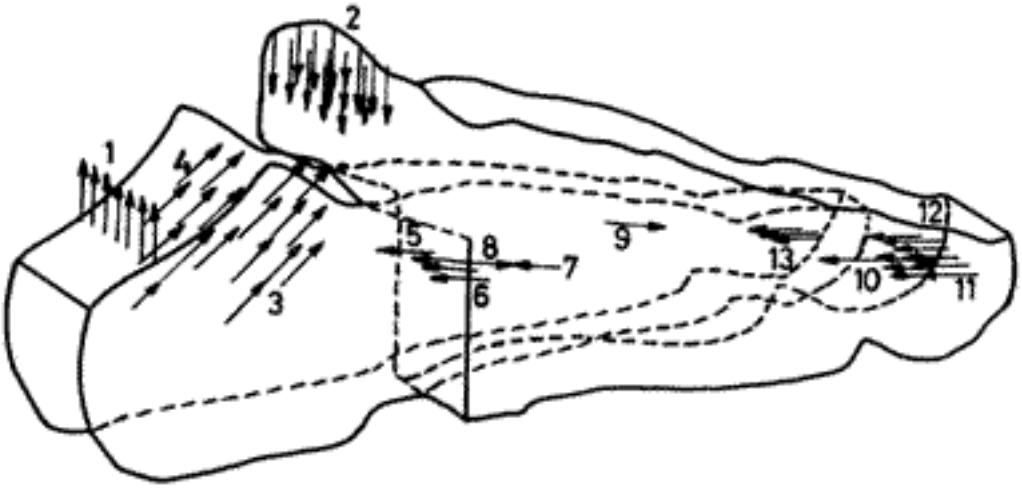


**Figure 3.**
Medial view of the two-arch foot model with plantar soft tissue in the mid-stance phase. Acting forces are indicated by numbers 1-13. 1=TS; 2=FAN; 3=reaction on the medial pulley due to FHL, FDL, and TP; 4=reaction on the lateral pulley due to PL and PB; 5=PB; 6=TP; 7=PL; 8=AH in medial arch; 9=AH in lateral arch; 10=AH in toe; 11=FHL; 12=FDL in medial arch; 13=FDL in lateral arch. Forces 1, 5-13 are distributed over thickness; the rest over area.

The forces on the calcaneus due to the muscles FHL, FDL, and TP, as they go around the medial pulley, and PL and PB, as they go around the lateral pulley, are also considered. The force in the muscle TS is taken from literature (16,36). The other muscle forces are calculated from the ratio of cross sectional areas of the muscles with respect to that of TS (37,38). The values of the muscle forces thus obtained compare well with those reported in literature (14,37). The lateral view of the FE mesh used in this model of the foot in the mid-stance phase is shown in **Figure 4.** The model has 3,292 brick elements representing bones, cartilages, and soft tissue, 116 spring elements to represent ligaments, and 4,403 nodes. The boundary conditions imposed in the mid-stance phase are: the displacements of the nodes of medial borders of the heel and metatarsal heads and toes of the medial and lateral arches are arrested in the x, y, and z directions; the lateral border nodes of the same regions are arrested for displacements in the x and y directions; and the other nodes on the heel and metatarsal heads and toes of the medial and lateral arches are arrested for the vertical displacements.

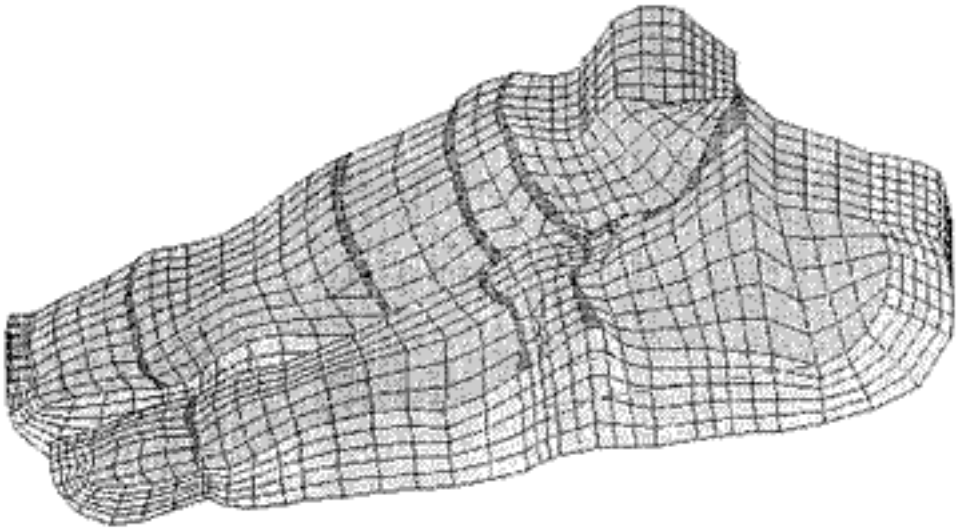

**Figure 4.**
Lateral view of the FE discretization of the two-arch model of the foot with plantar soft tissue in the mid-stance phase.

*Push-off Phase*

The push-off phase is characterized by a 45° inclination of the foot sole to the ground (34). The FAN is simulated by 5 times the body weight (35). The predominant muscle forces considered in this phase are TS, TP, PL, PB, FHL, and FDL (15,16). The forces at the medial pulley from FHL, FDL, and TP, and at the lateral pulley from PL and PB, are also considered, as shown in **Figure 5.** The forces in the above muscles are obtained from literature (16,36) and also by force equilibrium considerations (**Table 1**). The FE mesh used is similar to that shown in the mid-stance phase, with a finer mesh at the medial and lateral metatarsal head and toe regions. The model has 3,840 brick elements and 116 spring elements with 5,122 nodes and 15,366 degrees of freedom. The boundary conditions imposed are: the displacements of the nodes of the medial borders of metatarsal head and toe of the medial and lateral arches are arrested in the x, y, and z directions; the displacements of the nodes of the lateral borders of the same regions are arrested in the x and y directions; and the displacements of the other nodes in the above regions are arrested in the y direction.

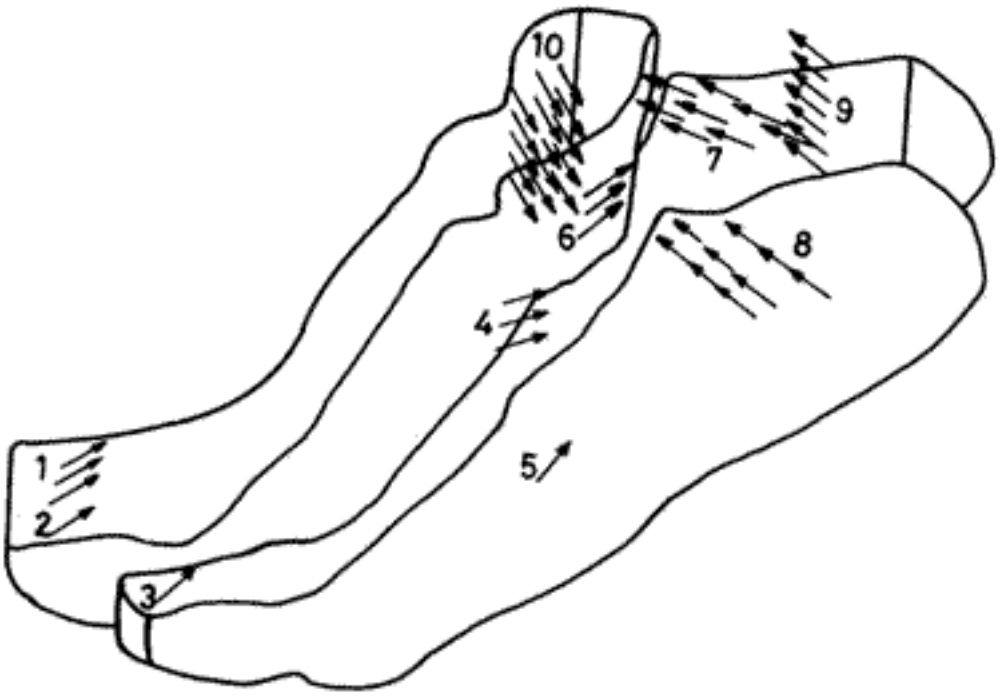


**Figure 5.**
Lateral view of the FE discretization of the two-arch model of the foot with plantar soft tissue in the push-off phase. Acting forces are indicated by numbers 1-10. 1=FHL; 2=FDL in medial arch; 3=FDL in lateral arch; 4=PL; 5=PB; 6=TP; 7=reaction on the medial pulley due to FHL, FDL, and TP; 8=reaction on the lateral pulley due to PL and PB; 9=TS; 10=FAN. Forces 1-6 and 9 are distributed over thickness; the rest over area.

**Foot Model in the Early Stage of Hansen's disease with Muscle Paralysis**

Since persons with HD have deformed feet, in addition to partial or complete paralysis of certain muscles, the analysis considers the shape of the foot from the X-ray and the muscle status (regarding the degree of muscle paralysis) from the clinical data. The left foot of subject CHN with drop foot from early stage HD is considered for the model. From the radiological assessment, it is seen that there is a reduction in thickness for the cartilages between talus and navicular, and navicular and cuneiforms. The X-ray data show a change in the geometry of the navicular known as beaking of the navicular bone. From clinical data it is found that intrinsic muscles and the peroneal muscles, PL and PB, are completely paralyzed. The dorsiflexor muscles TA, EHL, and EDL are also completely paralyzed, leading to drop foot. There is 20 percent (grade 4, see **Table 2**) paralysis for TP. Since the dorsiflexors are paralyzed, there exists no heel-strike phase; hence, only the mid-stance and push-off phases are modeled.

**Table 2.**

Muscle power grading as per Medical Research Council of Britain.

| Muscle Grading | Muscular Condition |
|---|---|

| | |
|---|---|
| 0 | No movement of the muscle. |
| 1 | Slight movement of the muscle. |
| 2 | Considerable movement and contraction in position toward gravity but not against gravity. |
| 3 | Considerable and appreciable contraction and movement both against and toward gravity. |
| 4 | Contraction and movement is good, but not against resistance. |
| 5 | Normal contraction and movement of the muscle. |

*Mid-stance Phase*

The foot is modeled as two arches with the inclusion of soft tissue of the foot sole. The mid-stance phase is simulated with the geometry obtained from medio-lateral and antero-posterior X-ray pictures of the foot. The paralyzed muscle forces are taken according to clinical report, and the remaining muscle forces are obtained from literature and by force equilibrium considerations (as in the earlier models). The normal values of forces for FHL, FDL, and TS are considered. The force in the TP is taken as 80 percent of the force in the normal foot model (per clinical report of 20 percent paralysis). The reaction on the medial side of calcaneus, due to TP, FHL, and FDL, is taken into account. Since the peroneal muscles PL and PB are paralyzed, there is no reaction force at the lateral side of calcaneus. The muscle forces and FAN acting on the foot of CHN are given in **Table 3.** The boundary conditions used are same as those described above for the same phase.

**Table 3.**

Muscle forces and ankle joint force acting on the two-arch foot model with soft tissue of the foot sole for the subject CHN (early stage of Hansen's disease) in the mid-stance and push-off phases of walking.

| | **Magnitude (N)** | |
|---|---|---|
| **Forces** | **Mid-stance** | **Push-off** |
| Ankle Joint Force (FAN) | 2,100 | 3,000 |

| | | |
|---|---|---|
| Triceps Surae (TS) | 550 | 1,361 |
| Peroneus Longus (PL) | 0 | 0 |
| Peroneus Brevis (PB) | 0 | 0 |
| Tibialis Posterior (TP) | 232 | 362 |
| Flexor Hallucis Longus (FHL) | 143 | 259 |
| Flexor Digitorum Longus (FDL) | 68 | 130 |
| Reaction at medial pulley due to muscle forces FHL, FDL, and TP | 574 | 560 |
| Reaction at lateral pully due to muscle forces PL and PB | 0 | 0 |

*Push-off Phase*

As explained in the earlier section, push-off phase is characterized by a 45° inclination of the foot sole to the ground. The muscle forces are modeled with normal values of FHL and FDL and 80 percent of TP. For the equilibrium of the foot in the push-off position, it is assumed that the powerful muscle TS generates more force than its normal value, and it is calculated. The reaction at the calcaneus due to the muscles FHL, FDL, and TP going around the medial pulley is modeled. The reaction at the lateral pulley is zero, because of the paralysis of lateral peroneal muscles. The forces in these muscles and the FAN used (considering equilibrium in push-off phase) for the model are shown in **Table 3.** The muscles are distributed over an area as per the anatomy (12-14). The model of the foot, in the push-off phase with the forces acting, is shown in **Figure 6.** The boundary conditions used are same as those explained above for the same phase.

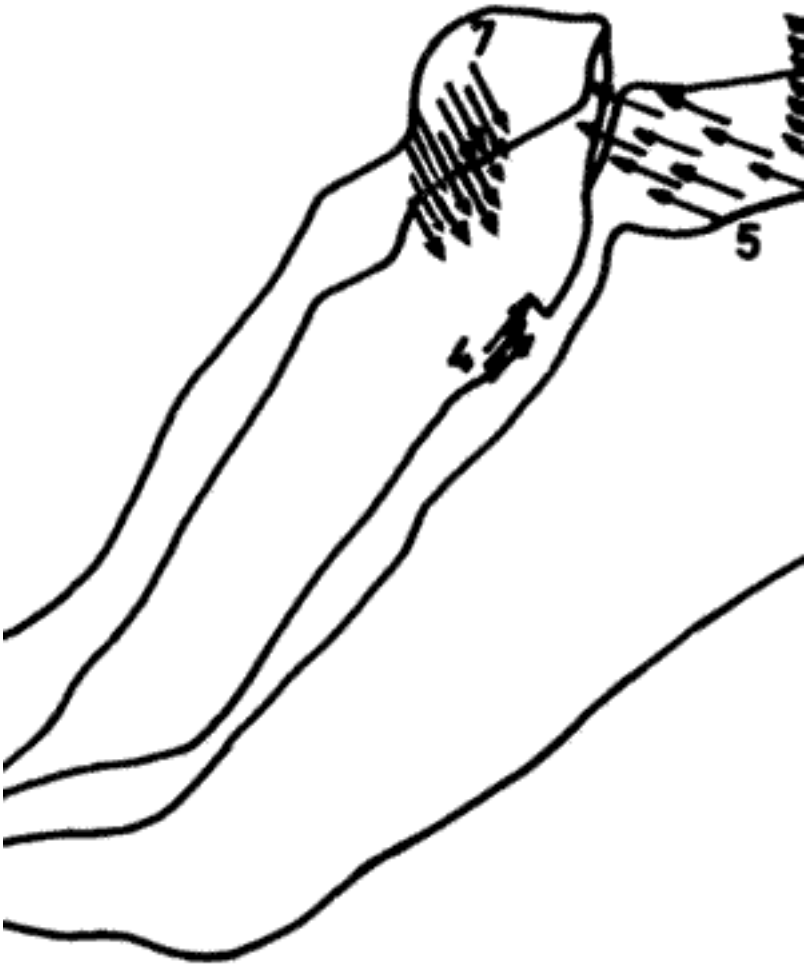


**Figure 6.**
Lateral view of the two-arch model of the foot with plantar soft tissue in the push-off phase for the subject CHN. Acting forces are indicated by numbers 1-7: 1=FHL; 2=FDL in medial arch; 3=FDL in lateral arch; 4=TP; 5=reaction on the medial pulley due to FHL, FDL, and TP; 6=TS; 7=FAN. Forces 1-4 and 6 are distributed over thickness; the rest over area.

## RESULTS

### Control Foot Model

*Heel-strike Phase*

From the stress analysis, it is found that the highest von Mises stress during heel-strike phase occurs at the lateral dorsal side of medial metatarsal head (4.1 MPa). The other regions of high stress or stress concentration are the dorsal medial side of the central part of the lateral metatarsals (3.8 MPa), the ankle joint (3.2 MPa), the medial side of medial metatarsals near the cartilage between cuneiforms and medial metatarsals (3.2 MPa), the dorsal medial side of the lateral toes (2.9 MPa), the dorsal junction of calcaneus and cuboid (2.3 MPa), the plantar anterior part of calcaneus at the insertion points of spring ligaments (2.3 MPa), and the neck of the talus (1.7 MPa). The highest von Mises stress (vertical component) at the interface between soft tissue and ground occurs at the medial anterior part of the heel region (0.35 MPa). It is found that this peak

stress at the plantar surface of the soft tissue (**Table 4**) is of the same order of magnitude as the peak pressure under the foot sole obtained by barographic measurements (39) for controls in heel-strike phase.

*Mid-stance Phase*

The results of stress analysis for the model in the mid-stance phase show that the maximum von Mises stress occurs at the dorsal side of the junction of calcaneus and cuboid (9.2 MPa). The other high stress/stress concentration regions are the ankle joint (6.6 MPa), the neck of the talus (4.6 MPa), the medial dorsal sides of the central parts of lateral and medial metatarsals (3.3 MPa), the dorsal side of navicular (3.3 MPa), and the medial plantar side of navicular (2.6 MPa). The maximum von Mises stress (vertical component) in the foot sole soft tissue at the foot/ground interface is 0.25 MPa (**Table 4**), which occurs at the first toe in the medial arch. This peak stress at the plantar surface of the soft tissue is of the same order of magnitude as the peak pressure under the foot sole obtained by barographic measurements (39) for a control during the mid-stance phase.

**Table 4.**

Comparison of peak foot sole stresses and experimentally measured foot pressures for control and Hansen's disease subject.*

| Subject | Phase of Walking | Model Stresses | Barographic Pressure |
|---|---|---|---|
| **Control** | Heel-strike | 0.35 | 0.30 |
| | Mid-stance | 0.25 | 0.22 |
| | Push-off | 0.50 | 0.45 |
| **CHN** | Mid-stance | 0.25 | 0.30 |
| | Push-off | 0.55 | 0.50 |

* From Patil, et al. (39). Note: The subject CHN, in early stage of Hansen's disease, could not have heel strike due to paralysis of dorsiflexors. Stresses and pressures in MPa.

*Push-off Phase*

The analysis of the model in the push-off phase shows that the maximum von Mises stress is at the dorsal medial side of central part of lateral metatarsals (21.5 MPa as shown in **Figure 7**). The other regions of high stress are the dorsal side of the junction of calcaneus and cuboid (19.9 MPa),

the lateral (16.9 MPa) and the medial (15.3 MPa) dorsal sides of the central part of the medial metatarsals, the neck of the talus bone (10.7 MPa) and the ankle joint (9.2 MPa).

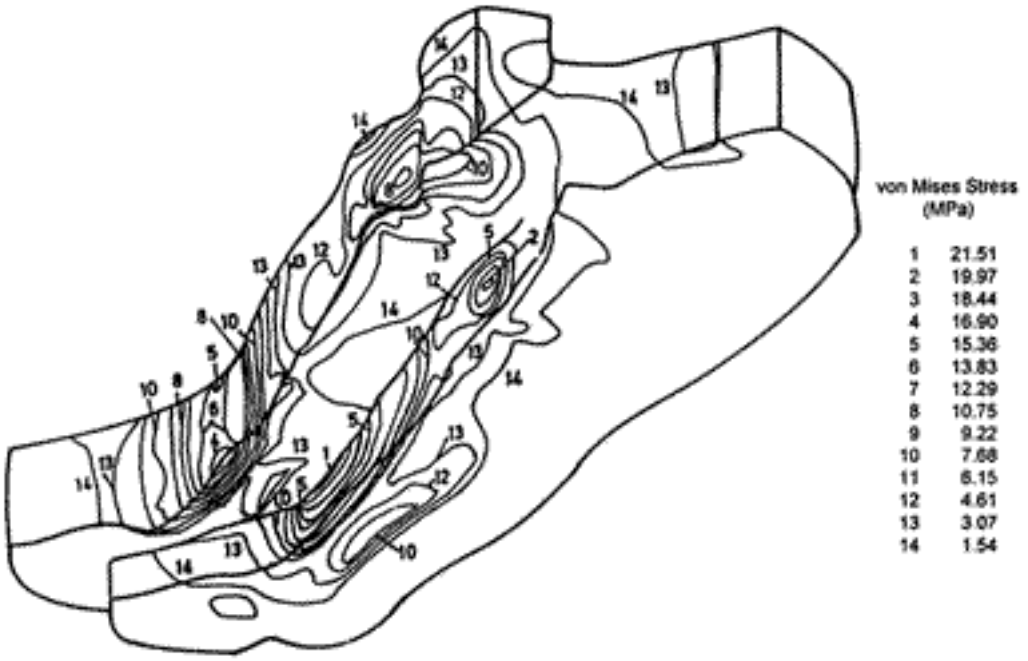


**Figure 7.**
Lateral view of the von Mises contours of the two-arch model of the foot with plantar soft tissue in the push-off phase.

The stresses in the cartilages are all compressive in nature with the highest (5 MPa) occurring in the cartilage between calcaneus and cuboid. The von Mises stress (vertical component) at the soft tissue/ground interface is found to be maximum at the central part of the lateral metatarsal head, possibly coinciding with the fourth metatarsal head (0.5 MPa). The highest von Mises stress in the medial arch is 0.5 MPa, which occurs at the lateral side of the metatarsal head, possibly coinciding with the third metatarsal head. The peak soft tissue stresses at the foot/ground interface (**Table 4**) are of the same order of magnitude as the peak pressures under the foot sole of controls reported in literature (40) and also obtained by barographic measurements (39). The results of stress analysis in the normal foot model, in three phases of walking are summarized and presented in **Table 5.**

**Table 5.**

Comparison of stresses in the control foot model in three phases of walking.

| Phase of Walking | von Mises Stress (MPa) | Stress concentration areas of the foot |
|---|---|---|

| | | |
|---|---|---|
| Heel-strike | 4.1 | Lateral dorsal side of medial metatarsal head |
| | 3.8 | Dorsal medial side of central part of lateral metatarsals |
| | 3.2 | Ankle joint, Medial side of medial metatarsals |
| | 2.9 | Dorsal medial side of lateral toes |
| | 2.3 | Dorsal junction of calcaneus and cuboid, Plantar anterior part of calcaneus |
| | 1.7 | Neck of talus |
| | 0.34 | Medial heel support (ground-soft tissue interface) |
| Mid-stance | 9.2 | Dorsal junction of calcaneus and cuboid |
| | 6.6 | Ankle joint |
| | 4.6 | Neck of talus |
| | 3.3 | Medial dorsal side of central part of lateral and medial metatarsals, dorsal side of navicular |
| | 2.6 | Plantar side of navicular |
| | 0.2 | First toe in the medial arch (ground-soft tissue interface) |
| Push-off | 21.5 | Dorsal medial side of central part of lateral metatarsals |
| | 19.9 | Dorsal junction of calcaneus and cuboid |
| | 16.9 | Dorsal lateral side of central part of medial metatarsals |
| | 15.3 | Dorsal medial side of central part of of medial and lateral metatarsals |
| | 10.7 | Neck of talus |
| | 0.5 | Plantar side of lateral metatarsal head (ground-soft tissue interface) |

**Early Stage of Hansen's Disease with Muscle Paralysis**

*Mid-stance Phase*

The highest stress during the mid-stance phase occurs at the dorsal side of the junction of calcaneus and cuboid (11.5 MPa). The other regions of high stress concentration are the ankle joint (6.5 MPa), the neck of the talus (4.1 MPa), the dorsal sides of the central part of medial (4.1 MPa), and lateral (3.3 MPa), metatarsals, and the navicular (3.3 MPa), as indicated in **Table 6.** By comparing the stresses in this model of CHN with that of controls for the mid-stance phase, it is found that the highest stress at the dorsal side of calcaneo-cuboid joint is increased by 25 percent. This could be due to the inversion of the foot from an imbalance of muscle forces between medial and lateral sides. The inversion could be because the lateral pulley force is absent, since the muscles going around the lateral pulley (PL and PB) are completely paralyzed, and there is force at the medial pulley due to muscle TP. The change in stresses, compared to those of the control foot in the other regions is not significant for the mid-stance phase. The stresses in the cartilages are compressive in nature in this case also. There is reduction in the thickness of the cartilages between talus and navicular, and navicular and cuneiforms; the compressive stresses in these cartilages are increased by 1.35 times and 1.27 times, respectively, compared to the values in the corresponding regions of the normal foot. The stresses in the other cartilages are nearly the same as those of the normal foot.

**Table 6.**

Comparison of foot bone von Mises stresses for CHN, in the early stage of Hansen's disease, with drop foot, in two phases of walking.

| Phase of Walking | von Mises Stress (MPa) | Stress concentration areas of the foot |
|---|---|---|
| Mid-stance | 11.5 | Dorsal junction of calcaneus and cuboid |
| | 6.5 | Ankle joint |
| | 4.1 | Neck of talus, Dorsal central part of medial metatarsals |
| | 3.3 | Dorsal central part of lateral metatarsals, Dorsal side of navicular |
| | 0.2 | Lateral toe (ground-soft tissue interface) |
| Push-off | 26.7 | Dorsal central part of lateral metatarsals |

| | |
|---|---|
| 24.8 | Dorsal junction of calcaneus and cuboid |
| 15.2 | Dorsal central part of medial metatarsals |
| 11.4 | Neck of talus, Plantar central part of lateral metatarsals |
| 7.6 | Dorsal side of navicular, Plantar side of medial and lateral toes, Dorsal side of cuneiform |
| 0.55 | Lateral side of medial and lateral metatarsal heads (ground-soft tissue interface) |

The highest von Mises (vertical component) stress (0.25 MPa) in the soft tissue/ground interface is found to be at the lateral toe (fourth toe region) and it is of the same order of magnitude as the measured foot pressure (**Table 4**). The other regions of high von Mises stresses are the heel (0.2 MPa), fourth metatarsal head (0.2 MPa), first toe (0.2 MPa) and medial metatarsal head (0.17 MPa).

*Push-off Phase*

**Table 6** presents a summary of stress analysis results in mid-stance and push-off phases for CHN. During the push-off phase, it is found that the highest von Mises stress occurs at the dorsal side of the central part of lateral metatarsals (26.7 MPa, **Figure 8**), which is 24 percent more than the stress at the same area for the normal foot. The other areas with high stresses are the dorsal side of the junction of calcaneus and cuboid (24.8 MPa), the dorsal side of the central part of the medial metatarsals (15.2 MPa), the neck of the talus (11.4 MPa) and the plantar side of the central part of the lateral metatarsals (11.4 MPa). The other regions of stress concentration are the dorsal side of navicular (7.6 MPa) and the dorsal side of cuneiform (7.6 MPa). The highest soft tissue von Mises stress (vertical component) at the foot sole/ground interface occurs at the lateral sides of the medial and lateral metatarsal heads (0.55 MPa), and it is of the same order of magnitude as the measured foot pressure (**Table 4**). The von Mises stresses (vertical component) at other regions of the foot sole are 0.47 MPa and 0.35 MPa, respectively, at the lateral sides of medial and lateral toes.

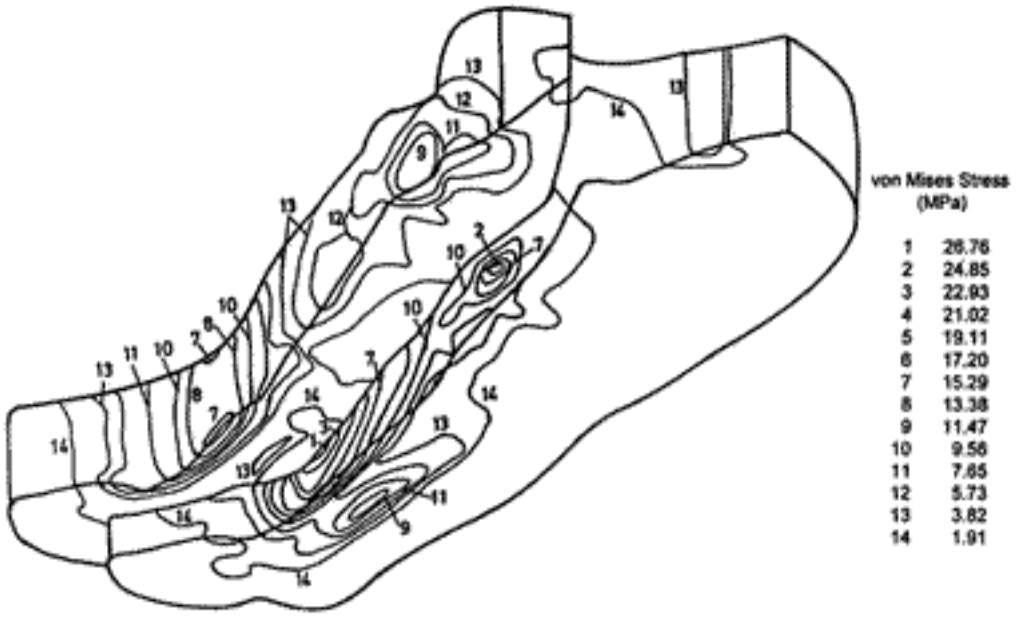


**Figure 8.**
Lateral view of the von Mises contours of the two-arch model of the foot with plantar soft tissue in the push-off phase for the subject CHN.

**Table 7** presents a comparison of bone von Mises stresses in controls and in CHN. The increase in stress (as seen here for CHN in the cuneiforms) to 7.6 MPa from 4.6 MPa (for the control foot in the corresponding area) could be because of the reduction in thickness of the cartilage between navicular and cuneiforms. During the push-off phase, the increase in stresses in the bones of the lateral arch is more than that of the bones of the medial arch. This could be due to the inversion of the foot caused by the imbalance in the muscle forces brought about by paralysis of lateral muscles, whereby more force is transferred to the lateral arch and subsequently to the ground. The stresses in the cartilages are compressive; the highest stress in the cartilage between talus and navicular is increased by 47 percent, and that of the cartilage between navicular and cuneiforms by 64 percent, of the corresponding cartilage stresses of the normal foot. The stresses in the other cartilages do not change significantly.

**Table 7.**

Comparison of foot bone von Mises stresses between foot models for control and CHN, an early stage Hansen's disease subject with drop foot in the push-off phase.

| Stress concentration areas of the foot | Control (MPa) | CHN (MPa) | Percent Change |
|---|---|---|---|
| Dorsal central part of lateral metatarsals | 21.5 | 26.7 | +24.1 |
| Dorsal junction of calcaneus and cuboid | 20.0 | 24.8 | +24.6 |

| | | | |
|---|---|---|---|
| Dorsal central part of medial metatarsals | 16.9 | 15.3 | -9.0 |
| Neck of talus | 10.7 | 11.5 | +7.0 |
| Plantar central part of lateral metatarsals | 7.7 | 11.5 | +49.7 |
| Dorsal side of navicular | 7.6 | 7.6 | -- |
| Plantal side of medial toes | 6.1 | 7.6 | +24.4 |
| Dorsal side of cuneiforms | 4.6 | 7.6 | +65.9 |

## DISCUSSION

Models reported in literature differ with respect to the number of segments defined, the number of dimensions considered, the number of muscles included, and the algorithms used to solve the stresses. Additionally, the anatomical information and the material properties used in the different models are not identical. Consequently, it is difficult to compare the results of different models directly.

Nakamura et al. (1) show that the maximum compressive stress in the bone at the metatarsal head region is 0.90 MPa at the bone/soft tissue interface during the mid-stance phase. The present study gives the maximum von Mises stress at the metatarsal head region as 1.3 MPa at this interface and phase. The former model is two-dimensional, representing the foot as a single bone without considering the muscle forces. The difference in the results could be explained as due to the differences in the geometry and muscles considered between the models. The plantar soft tissue stresses at the foot/ground interface are in good agreement with those measured by barographic equipment for all the three phases of walking (39).

The results of the stress analysis reported here show that the foot skeletal bone is subjected to the highest stress during the push-off phase of walking. During heel-strike, the highest von Mises stress (4.1 MPa) occurs at the lateral dorsal side of the medial metatarsal head, and the other regions of high stress concentrations are the dorsal medial side of the central part of the lateral metatarsals, the ankle joint, the medial side of medial metatarsals near the cartilage between cuneiforms and medial metatarsals, the dorsal medial side of lateral toes, the plantar anterior part of calcaneus at the insertion points of spring ligaments, the dorsal junction of calcaneus and cuboid and the neck of the talus. In the mid-stance phase the highest von Mises stress (9.2 MPa) occurs at the dorsal side of the junction of calcaneus and cuboid; the other areas of high stress concentration are the ankle joint, the neck of the talus, and the medial dorsal sides of the central part of lateral and medial metatarsals. The highest von Mises stress (21.5 MPa) during the push-off phase occurs at the dorsal medial side of the central part of the lateral metatarsals; the other areas of high stress concentrations are the dorsal side of the junction of calcaneus and cuboid, the lateral and medial dorsal sides of the central part of the medial metatarsals, and the neck of the talus. The highest von Mises stresses in the bones for the three phases of walking are in the ratio

HS:MS:PO=1:2.3:5.3 for the two-arch control foot model.

CHN does not have a heel-strike because of paralysis of dorsiflexors. From **Table 7** it is seen that this subject's highest von Mises stress in push-off occurs at the dorsal side of the central part of lateral metatarsals (26.7 MPa), 24 percent more than that of the control foot model at the same area. The increase in stress in the cuneiforms for CHN (7.6 MPa, 1.7 times that of the control) could be because of the reduction in the thickness of the cartilage between navicular and cuneiforms. For CHN in the push-off phase, the increase in stresses in the bones of the lateral arch is more than that of the medial arch. This could be due to the inversion of the foot because of the imbalance in muscle forces brought about by the paralysis of the lateral muscles (PL and PB). The early stage of HD (with reduction in cartilage thicknesses) has increased cartilage stresses by 47 to 64 percent in the corresponding areas. The paralysis of peroneal muscles (drop foot), combined with decreased cartilage thicknesses, has increased the bone stresses in push-off, in different parts of the foot, by 24 to 66 percent as described in **Table 7.**

## CONCLUSIONS

The results of the stress analysis show that the plantar soft tissue stresses at the foot/ground interface are in good agreement with the foot pressures (39) measured by barographic equipment for all the three phases of walking. The analysis for the control and HD foot shows that the bone areas of high stress concentration are the dorsal and plantar central parts of lateral metatarsals, the dorsal junction of calcaneus and cuboid, the dorsal central part of medial metatarsals, the neck of the talus, and the dorsal sides of navicular and cuneiforms in the push-off phase. The paralysis of peroneal muscles (drop foot), combined with decreased cartilage thicknesses in the early stage of HD, further increases the bone stresses in the push-off phase in the high-stress concentration regions of the foot by 24 to 66 percent. This is of great importance, since it is found from clinical reports (41) that in certain persons with HD, these areas of the bones get disintegrated if subject to osteoporosis, due to decreased mechanical strength of the bone in that region (caused by HD). Therefore, this investigation could possibly provide an insight into the factors contributing to tarsal disintegration in HD.

### ACKNOWLEDGMENT

The authors gratefully acknowledge the help given by Dr. P.K. Oommen, Joint Director, Central Leprosy Teaching and Research Institute, Chengalpattu, in providing the necessary radiographic and clinical details of the HD subjects.

### REFERENCES

1. Nakamura S, Crowninshield RD, Cooper RR. An analysis of soft tissue loading in the foot: a preliminary report. Bull Prosthet Res 1981;10-35(18):27-34.
2. Reddy NP, Pohit G, Lam PC, Grotz RC. Finite element modelling of ankle-foot orthoses. Proceedings of the International Conference on Biomechanics and Clinical Kinsiology of Hand and Foot; 1985, Madras, Indian Institute of Technology. p. 97-9.
3. Patil KM, Braak LH, Huson A. Stresses in a simplified two dimensional model of a normal foot: a preliminary analysis. Mech Res Commun 1993;20:1-7.
4. Patil KM, Braak LH, Huson A. A two-dimensional model of a normal foot with cartilages and ligaments for stress analysis. Innov Technol Biol Med 1993;14:152-62.
5. Rubricius D, Kraténa J. Numerical and photoelastic research of arthrodesis of the ankle. Proceedings of the Second World Congress of Biomechanics; 1994, Amsterdam, The Netherlands. p. 228.
6. Ploeg HL, Cooke TDV, Dujovne AR, Smith CM, Wyss UP. A three-dimensional finite element analysis in the development of a total joint replacement for the great toe (Abstract). J Biomech 1992;25:672.
7. Cavanagh PR, Hewitt Jr FG, Perry JE. In-shoe plantar pressure measurement: a review. Foot 1992;2:85-194.
8. Yettram AL, Camilleri NN. The forces acting on the human calcaneus. J Biomed Eng 1993;15:46-50.
9. Shorten MR. Finite element modeling of sports shoe cushioning. Proceedings of the Second World Congress of Biomechanics; 1994, Amsterdam, The Netherlands. p. 147.
10. Chu T-M, Reddy NP. Stress distribution in the ankle-foot orthosis used to correct pathological gait. J Rehabil Res Dev 1995;32(4):349-60.
11. Chu T-M, Reddy NP, Padovan J. Three-dimensional finite element stress analysis of the polypropylene, ankle-foot orthosis: static analysis. Med Eng Phys 1995;17:372-9.
12. McMinn RMH, Hutchings RT, Logan BM. A colour atlas of foot and ankle anatomy. London: Wolfe Medical Publications Ltd.; 1989.
13. Williams PL, Warwick R, Dyson M, Bannister LH. Gray's anatomy. 37th ed. New York: Churchill and Livingstone; 1989.
14. Kapandji A. The physiology of the joints. Vol. 2-lower limb. London: E & S Livingstone; 1970.
15. Basmajian JV. Muscles alive--their function revealed by electromyography. Baltimore: Williams and Wilkins; 1978.
16. Seireg A, Arvikar RJ. The prediction of muscular load sharing and joint forces in the lower extremities during walking. J Biomech 1975;8:89-102.
17. Scott SH, Winter DA. Talocrural and talocalcaneal joint kinematics and kinetics during the stance phase of walking. J Biomech 1991;24:743-52.
18. DeClercq D, Aerts P, Kunnen M. The mechanical characteristics of the human heel pad during foot strike in running: an in vivo cineradiographic study. J Biomech 1994;27:1213-22.
19. Huiskes R, Chao EYS. A survey of finite element analysis in orthopadic biomechanics: the first decade. J Biomech 1983;16:385-409.
20. Keaveny TM, Guo XE, Wachtel EF, McMahon TA, Hays WC. Trabecular bone exhibits fully linear elastic behaviour and yields at low strains. J Biomech 1994;27:1127-36.
21. Keaveny TM, Wachtel EF, Guo XE, Hays WC. Mechanical behaviour of damaged trabecular bone. J Biomech 1994;27:1309-18.

22. Reilly DT, Burstein AH, Frankel VH. The elastic modulus for bone. J Biomech 1974;7:271-5.
23. Reilly DT, Burstein AH. The elastic and ultimate properties of compact bone tissue. J Biomech 1975;8:393-405.
24. Fondrk M, Bahniuk E, Davy DT, Michaels C. Some viscoplastic characteristics of bovine and human cortical bone. J Biomech 1988;21:623-30.
25. Yamada H. Strength of biological materials. Baltimore: Williams and Wilkins; 1970.
26. Clift SE. Finite element analysis in cartilage biomechanics. J Biomed Eng 1992;14:217-21.
27. Woo SLY, Gomez MA, Woo YK. Mechanical properties of tendons and ligaments II: the relationships of immobilisation and exercise on tissue remodelling Biorheology 1982;19:397-408.
28. Schreppers GJMA, Sauren AAHJ, Huson A. A numerical model of the load transmission in the tibio-femoral contact area. Proc Inst Mech Eng (H) 1990;204:53-9.
29. Bennet L. Transferring load to flesh. Part II: analysis of compressive stress. Bull Prosthet Res 1971;10-16;45-63.
30. Bennet L. Transferring load to flesh. Part III: analysis of shear stress. Bull Prosthet Res 1972;10-17:38-51.
31. Bennet L. Transferring load to flesh. Part IV: flesh reaction to contact curvature. Bull Prosthet Res 1972;10-18:60-7.
32. Shiang TY, Cavanagh PR. Finite element analysis of the foot-shoe interface in diabetic patients. Proceedings of the Symposium on Biomedical Engineering in the 21st Century; 1992, Taipei, Taiwan, R.O.C. p. 1-7.
33. Zienkiewicz OC. The finite element method. 3rd ed. London: McGraw Hill; 1977.
34. Inman VT, Ralston HJ, Todd F. Human walking. Baltimore: Williams and Wilkins; 1981.
35. Røhrle HL, Scholten R, Sigolotto C, Sollbach W. Joint forces in the human pelvis-leg skeleton during walking. J Biomech 1984;17:409-24.
36. Calderale PM, Scelfo G. A mathematical model of the locomotor apparatus. Eng Med 1987;16:147-61.
37. Spoor CW. Mechanical models of selected parts of the human musculoskeletal system (thesis). Eindhoven, The Netherlands: Eindhoven University of Technology; 1992.
38. Crowninshield RD, Brand RA. A physiologically based criterion of muscle force prediction in locomotion. J Biomech 1981;14:793-801.
39. Patil KM, Babu M, Oommen PK, Malaviya GN. On line system of measurement and analysis of standing and walking foot pressures in normals and patients with neuropathic feet. Innov Technol Biol Med 1996;17:401-8.
40. Rosenbaum D, Hautmann S, Gold M, Claes L. Effects of walking speed on plantar pressure patterns and hind foot angular motion. Gait Posture 1994;2:191-7.
41. Kulkarni VN, Mehta JM, Sane SB, Sharangpani RC. Study of tarsal disintegration in leprosy. Proceedings of the International Conference on Biomechanics and Clinical Kinsiology of Hand and Foot; 1985, Madras, Indian Institute of Technology; 1985. p. 121-4.

Contents

Back to Top